Beam Fluorescence-based Beam Diagnostic Tomography

High Intensity Proton Beam Diagnostics workshop- September 27th

Cherry May Mateo- DITANET, CEA Saclay

Non-destructive diagnostics

Motivation

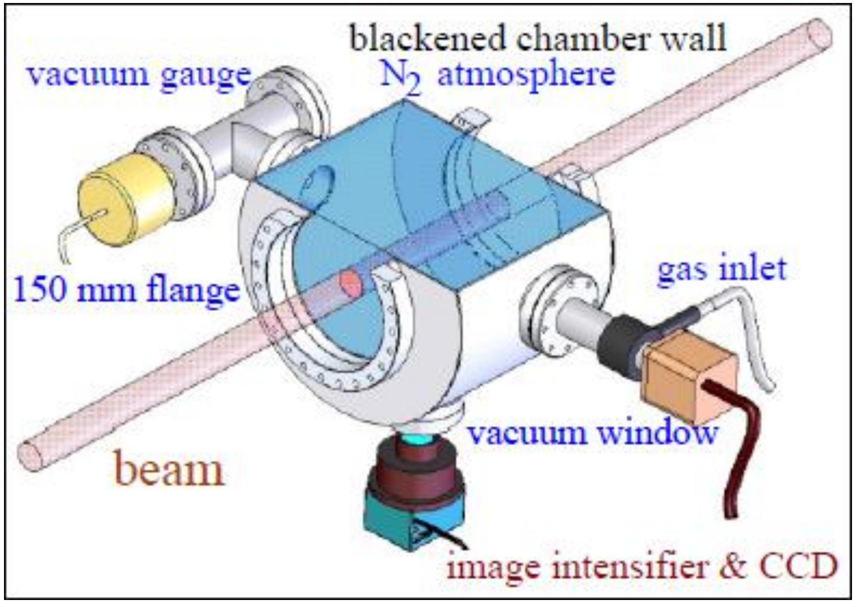

Schematic of BIF at GSI*

Increased demand

- It must not perturb the beam
- It must not be destroyed by **high current beam** (kilowatt beam power)

Optical Profilers

- Beam Induced Fluorescence (BIF) Monitor at GSI*
- Beam Ionization Optical profile monitors

*F. Becker et al., Beam Induced Fluorescence Monitor for Transverse Profile Determination of 5 to 750 MeV/u Heavy Ion Beams, Proceedings of DIPAC 2007, Venice, Italy

Objectives

- Discuss an overview of optical profile monitors
- Demonstrate that tomographic reconstruction can be incorporated with optical profilers to reconstruct beam's spatial density.

energie atomique • energies alternatives

Optical Profiler

Beam Fluorescence on residual gas

$$N_{photons} = K \cdot \Psi \cdot \rho \cdot \Delta s \cdot \sigma_{rad}$$

Radiative decay
hν in visible light

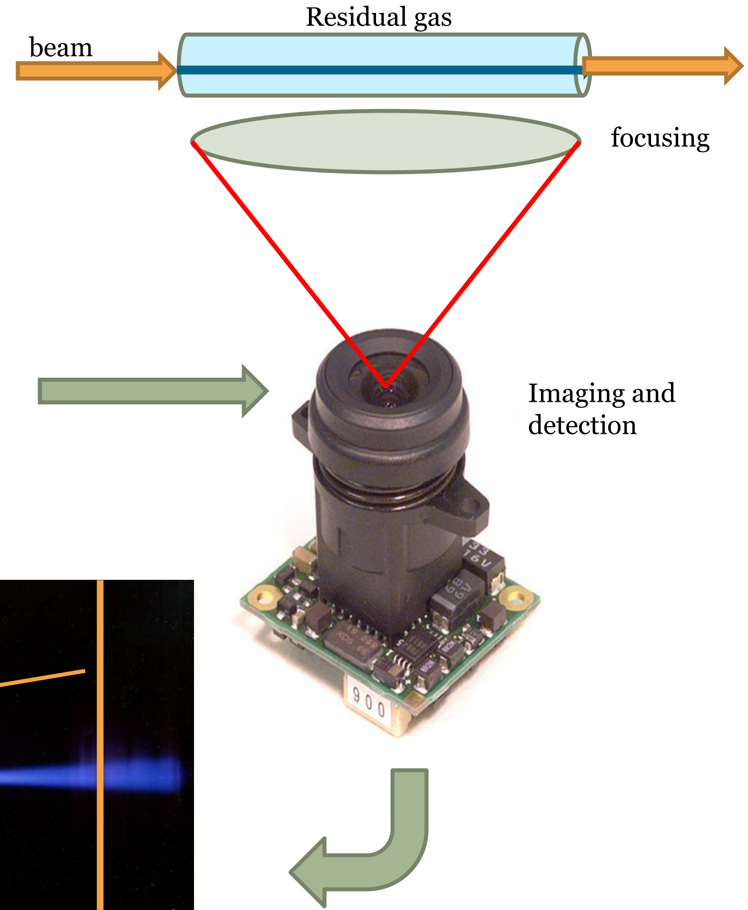

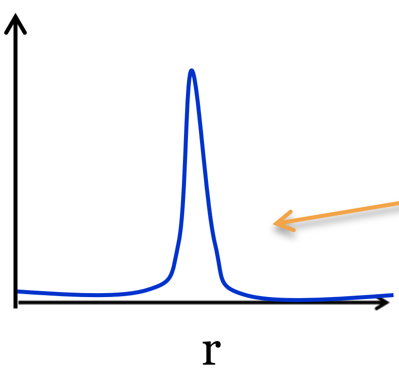

Image*

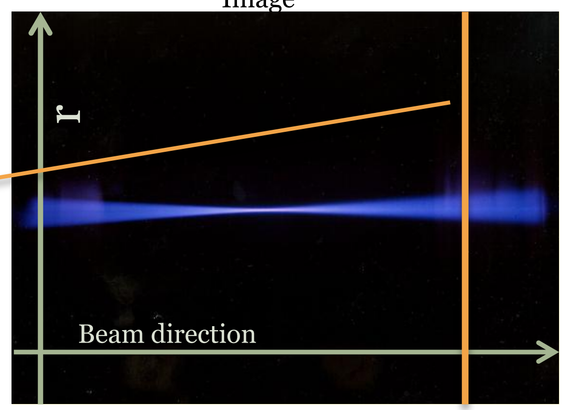

*Pottin, B, (2001) Etude d'un profileur optique de faisceaux intenses de protons par absorption laser, Doctor of Science thesis. Institut de Physique Nucléaire

Detectors

- 1D sensors
  - Photo diodes
  - Linear CCD arrays
  - Segmented photomultiplier
- 2D sensors
  - Area CCD arrays
  - Area CMOS
- Photocathode-based
  - Photomultiplier tubes
  - Image intensifiers
  - Segmented photomultiplier
- Solid state devices
  - APDs
  - CMOS
  - EMCCDs

Image Intensifiers

Image intensifiers converts photons into electrons, multiply them, and then convert them back into photons, maintaining spatial information.

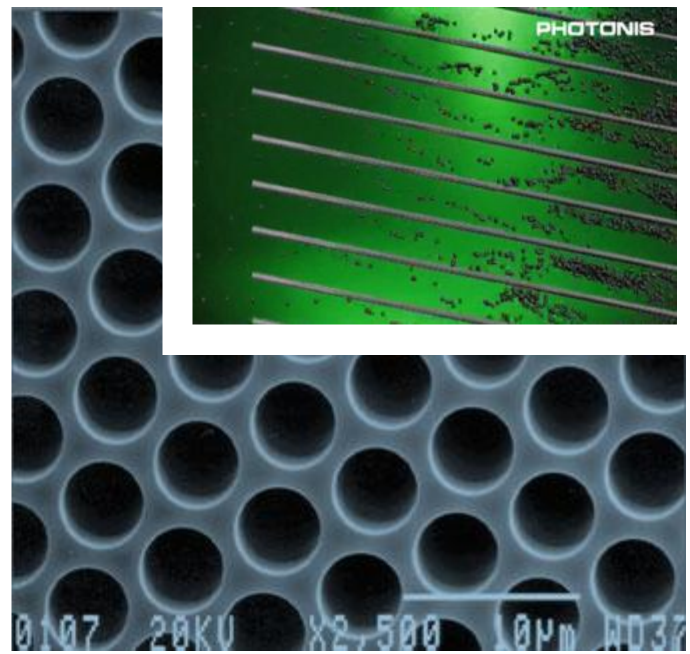

*Peter Seitz and Albert JP Theuwissen. *Single-Photon Imaging*.Heidelberg; Springer, 2011.

Optical Profiler in IPN/CEA

Beam profiles of proton beam

- ✓ Intensified CCD camera was used to capture beam image.
- ✓ No ion separation

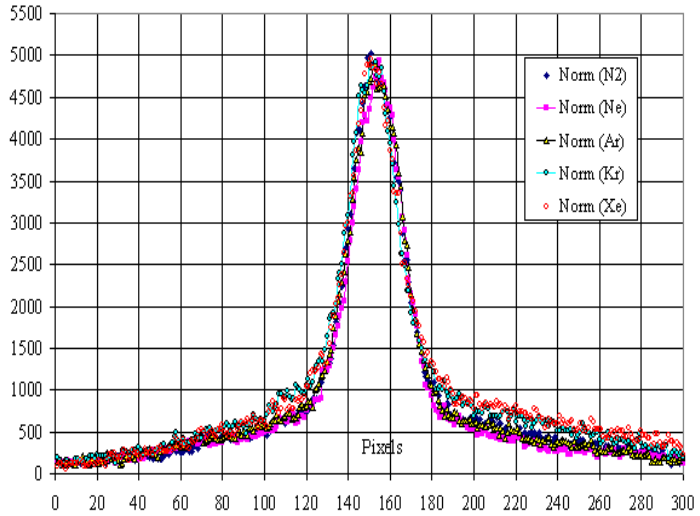

Profiles obtained with different gases but with constant gas pressure.

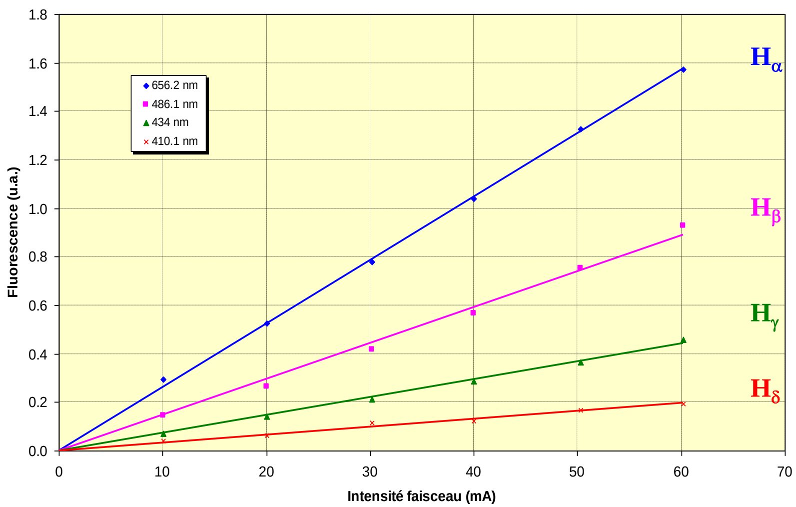

$$I_{lum} = I_{beam} \cdot \sigma \cdot n_0$$

*P. Ausset, et. al., *Transverse Beam Profile Measurements for High Power Proton Beams,* Proceedings of EPAC 2001, Paris, France

*Pottin, B, (2001) Etude d'un profileur optique de faisceaux intenses de protons par absorption laser, Doctor of Science thesis. Institut de Physique Nucléaire

Optical Profiler in IPN/CEA

Doppler Shift Spectroscopy allows discrimination of different beam components

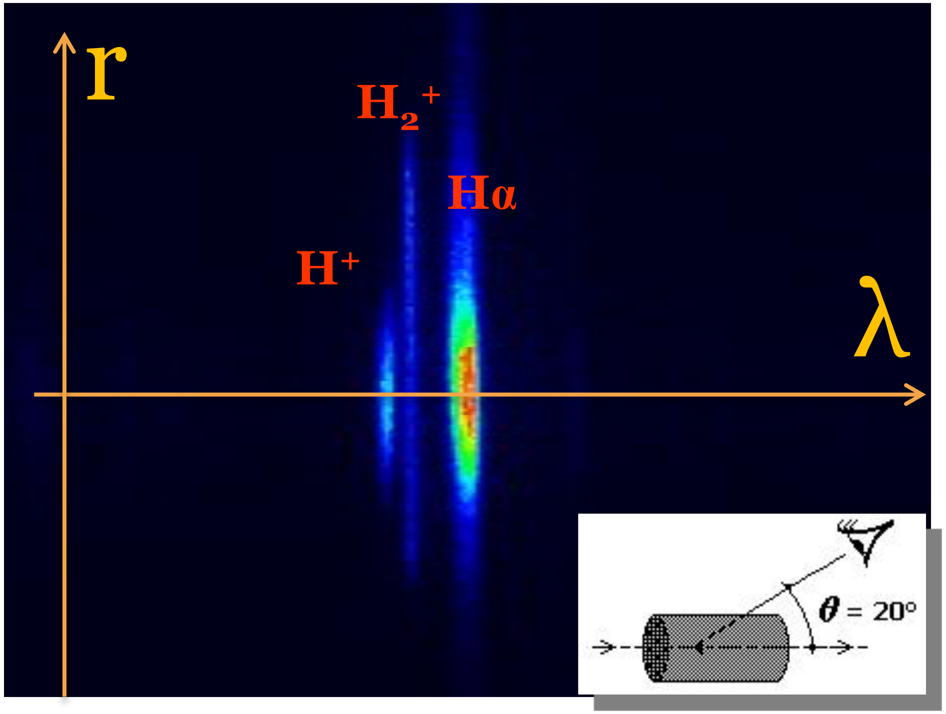

$$\Delta\lambda \approx \lambda_0 \, {}^{v}\!/_{c} \cos\theta$$

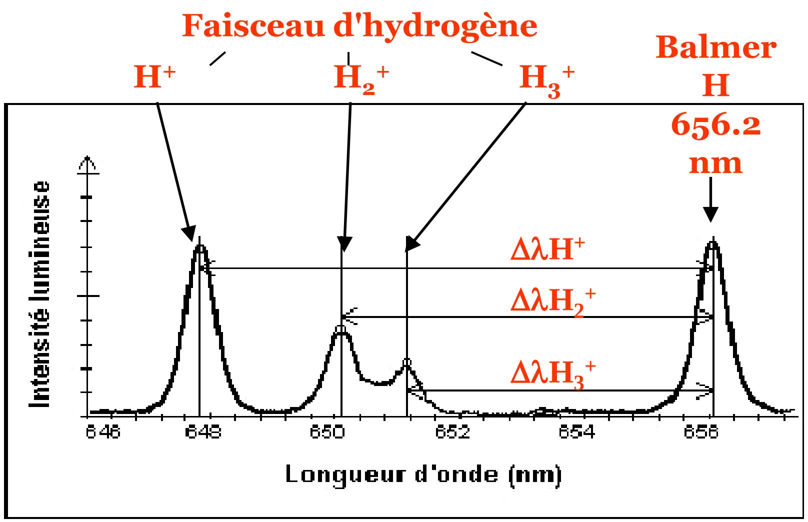

*Pottin, B, (2001) Etude d'un profileur optique de faisceaux intenses de protons par absorption laser, Doctor of Science thesis. Institut de Physique Nucléaire

*P. Ausset, et. al., *Transverse Beam Profile Measurements for High Power Proton Beams,* Proceedings of EPAC 2001, Paris, France

Beam fluorescence monitors allow multiple measurements of beam projections at different angles around the beam

Tomography

Has advantage when dealing with beam shapes that are more intricate.

Tomography

Tomography is the method used to reconstruct a 2D cross sectional image of an object given multiple flat scans taken from multiple angles around an object

Measurable (I HAVE) → $g(s, \theta_1)$, $g(s, \theta_2)$

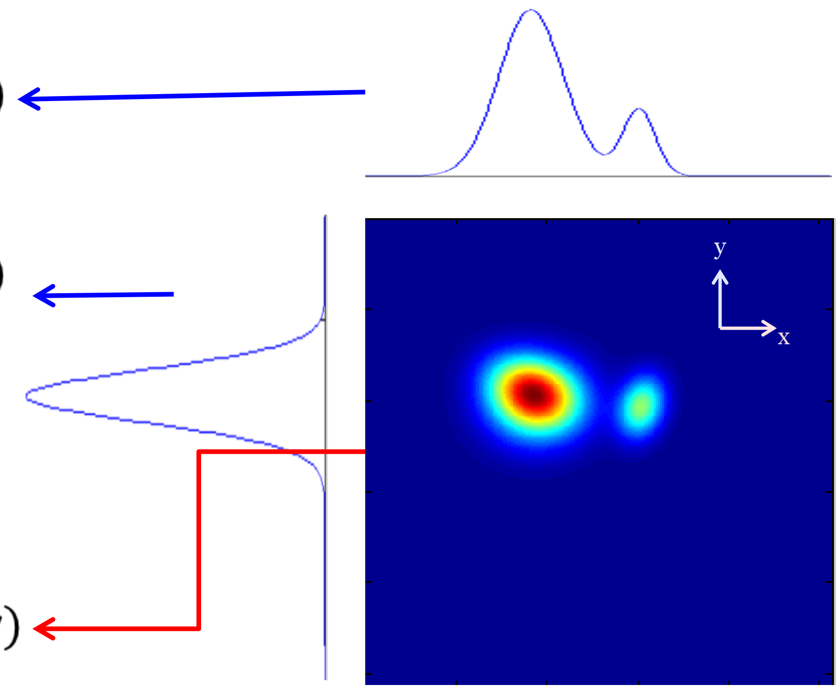

Solvable (I WANT) ← $f(x, y)$

Tomography

By Fourier Slice Theorem, EXACT value of *f(x,y)* can be calculated given an infinite number of projections

$$g_n(s) = \int_{-\infty}^{+\infty} f(x_n(s,t)\,,\, y_n(s,t))dt$$

$$= \int_{-\infty}^{+\infty} f(s\cos\theta - t\sin\theta,\, s\sin\theta + t\cos\theta)dt$$

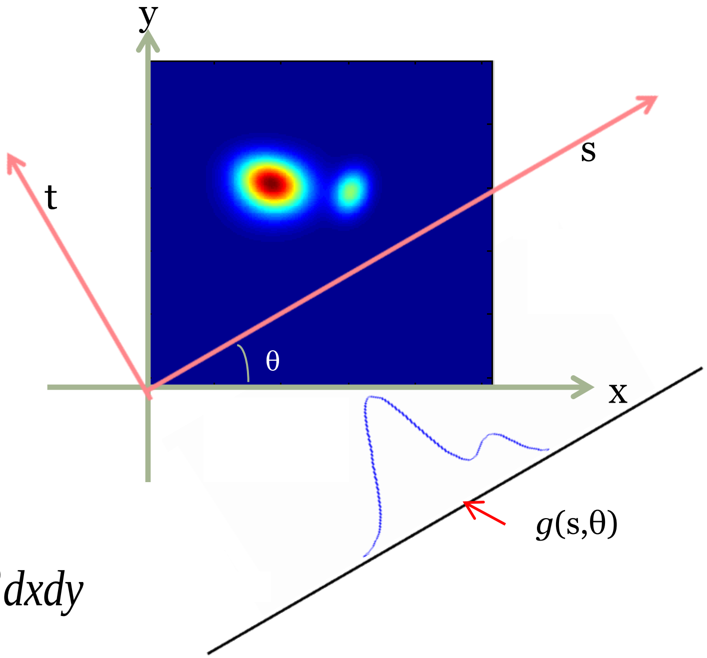

Fourier Slice theorem:

$$\int_{-\infty}^{+\infty} g(s,\theta)e^{-j2\pi\nu t}dt = \int_{-\infty}^{+\infty}\int_{-\infty}^{+\infty} f(x,y)e^{-j2\pi(\nu\cos\theta x+\nu\sin\theta y)}dxdy$$

How?

Algebraic Reconstruction Technique for 2 Projections

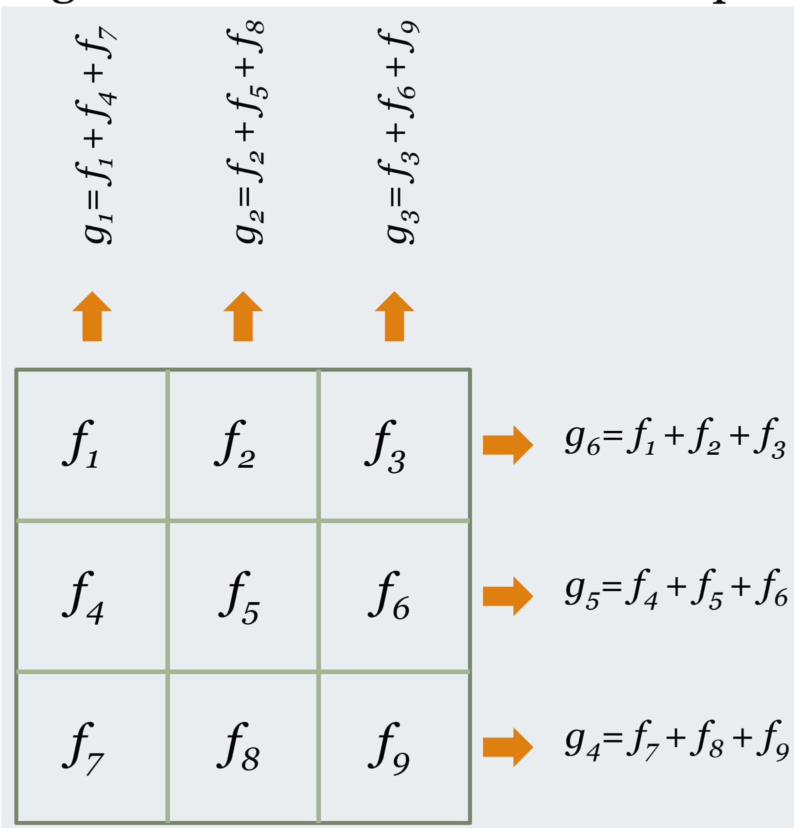

$$
\begin{cases}
g_1 = f_1 + f_4 + f_7 \\
g_2 = f_2 + f_5 + f_8 \\
g_3 = f_3 + f_6 + f_9 \\
g_4 = f_7 + f_8 + f_9 \\
g_5 = f_4 + f_5 + f_6 \\
g_6 = f_1 + f_2 + f_3
\end{cases}
$$

$$
\underbrace{\begin{bmatrix} g_1 \\ g_2 \\ g_3 \\ g_4 \\ g_5 \\ g_6 \end{bmatrix}}_{\boldsymbol{g}} = \underbrace{\begin{bmatrix} 1 & 0 & 0 & 1 & 0 & 0 & 1 & 0 & 0 \\ 0 & 1 & 0 & 0 & 1 & 0 & 0 & 1 & 0 \\ 0 & 0 & 1 & 0 & 0 & 1 & 0 & 0 & 1 \\ \hline 0 & 0 & 0 & 0 & 0 & 0 & 1 & 1 & 1 \\ 0 & 0 & 0 & 1 & 1 & 1 & 0 & 0 & 0 \\ 1 & 1 & 1 & 0 & 0 & 0 & 0 & 0 & 0 \end{bmatrix}}_{\boldsymbol{A}} \underbrace{\begin{bmatrix} f_1 \\ f_2 \\ f_3 \\ f_4 \\ f_5 \\ f_6 \\ f_7 \\ f_8 \\ f_9 \end{bmatrix}}_{\boldsymbol{f}}
$$

Projections — Sparse Matrix — Image

How?

Algebraic Reconstruction Technique for more than 2 projections

Sparse matrix for more projection angles not equal to 0˚ and 90 ˚

$$g_7 = C_4 f_4 + C_1 f_1 + C_2 f_2 + C_3 f_3$$

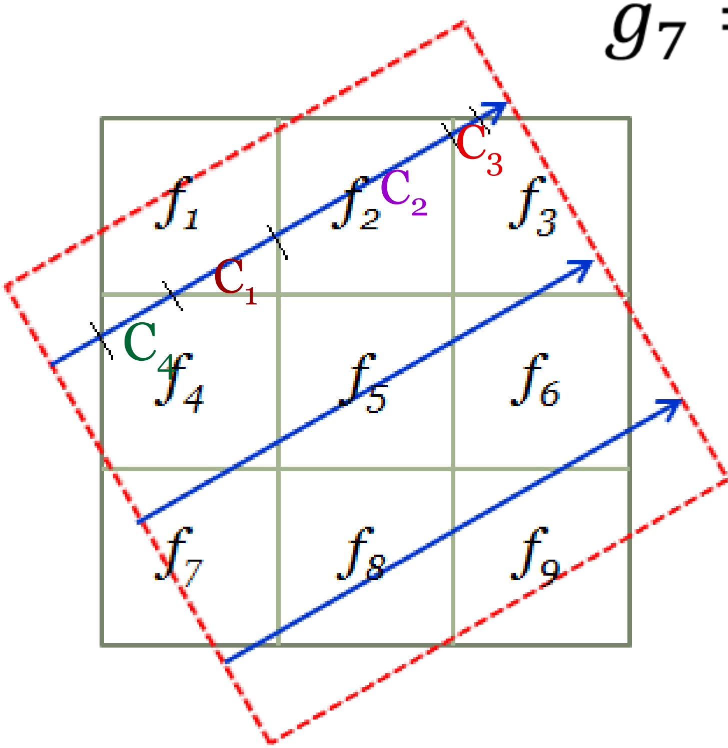

More angles ➔ more complicated sparse matrix

Number of rows

$= \textit{length of one projection} \times \textit{number of projections}$

Number of columns

$= (\textit{length of one projection})^2$

How?

Interested in finding a vector solution *f* to the vector equation:

$$g = Af$$

- f → unknown slice vector
- A → Sparse matrix or forward projection matrix
- g → Projection data vector

Iterative Procedure

How?

Iteration process

$$\overline{f}_j^{(k+1)} = \frac{\overline{f}_j^{(k)}}{\sum_{i=1}^{n} a_{ij}} \sum_{i=1}^{n} \frac{g_i}{\sum_{j'=1}^{m} a_{ij'} \overline{f}_{j'}^{(k)}} a_{ij}$$

- g Vector of projection data
- f Vector of unknown slice data
- A Matrix such that $g = Af$
- a_{ij} Value of element located at the i^{th} and j^{th} column of matrix A
- i Projection subscript
- j Pixel subscript
- g_i Number of counts in the i^{th} bin of the projection dataset
- m Number of pixels
- n Number of bins

$$Image^{(k+1)} = Image^{(k)} \times Normalized\ \ Backprojections\ \ of \left(\frac{Measured\ \ projections}{Projections\ \ of\ \ image^{(k)}} \right)$$

How?

Iteration process

Reducing error between calculated and initial Measurements

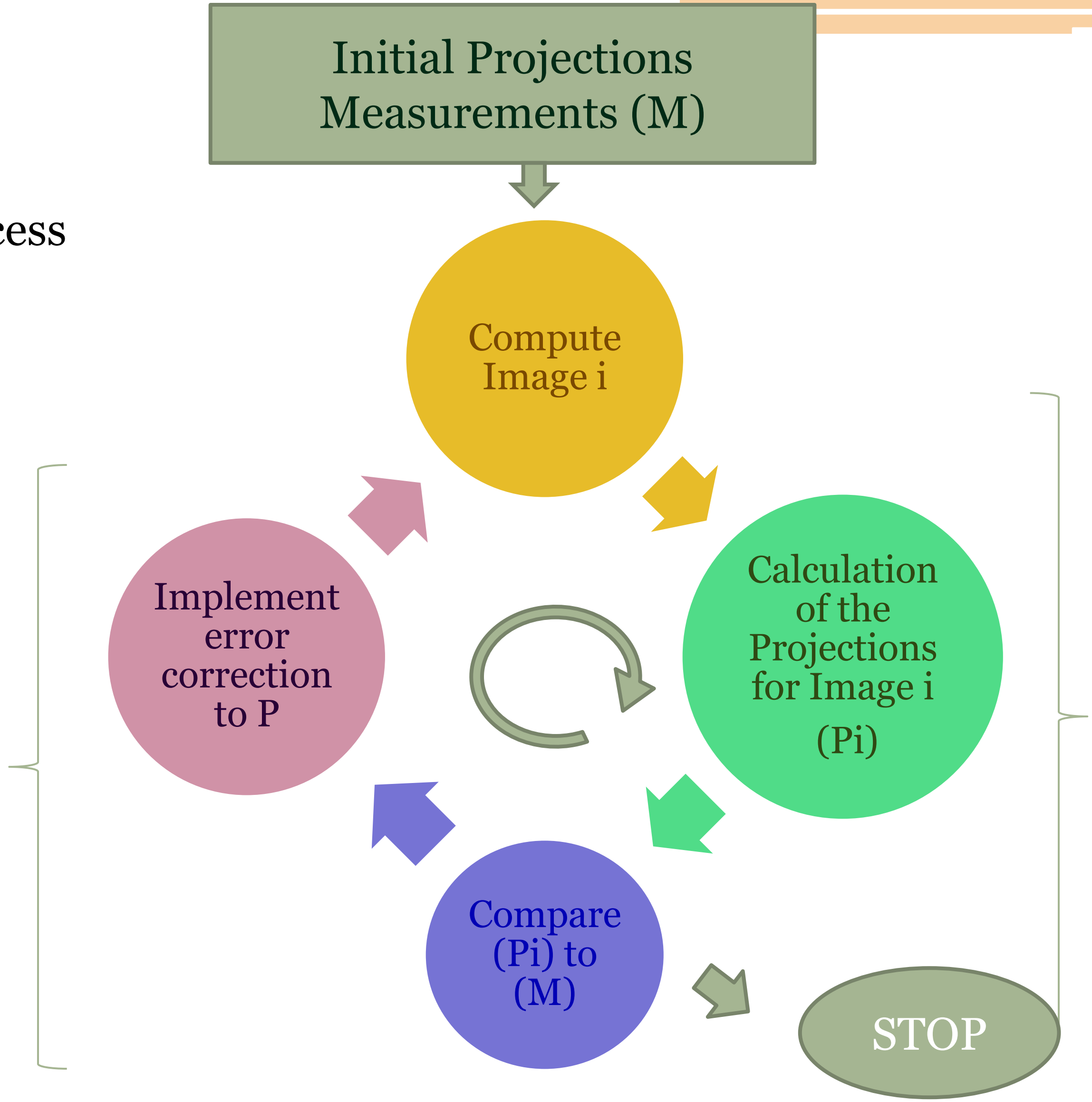

Processing and comparison

What?

Advantages of Algebraic Iterative technique:

Mathematical model that describes how the projections are obtained

- ✓ Physics of detection
- ✓ Scattering
- ✓ Pixel defects
- ✓ etc

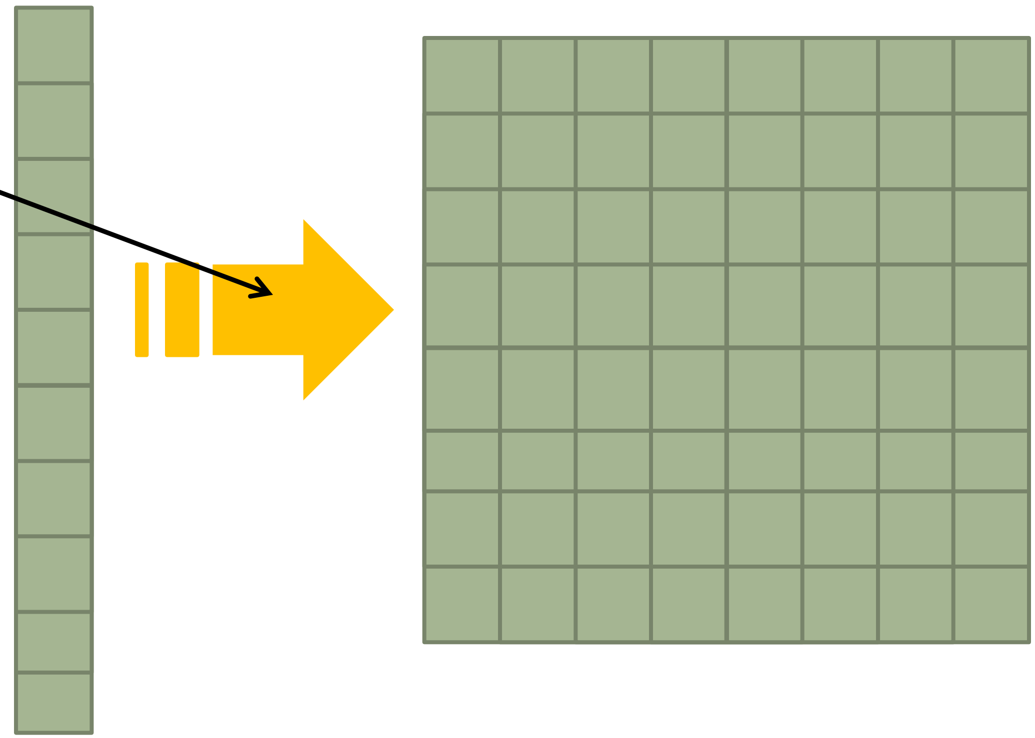

Projection plane

Image plane

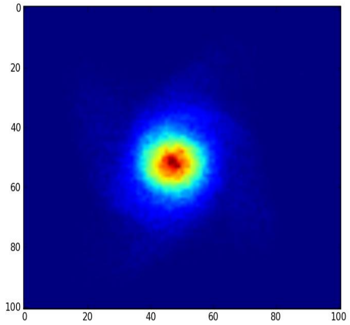

Numerical Illustration with MATLAB

Step 1

Image to Projections of the TEST IMAGE

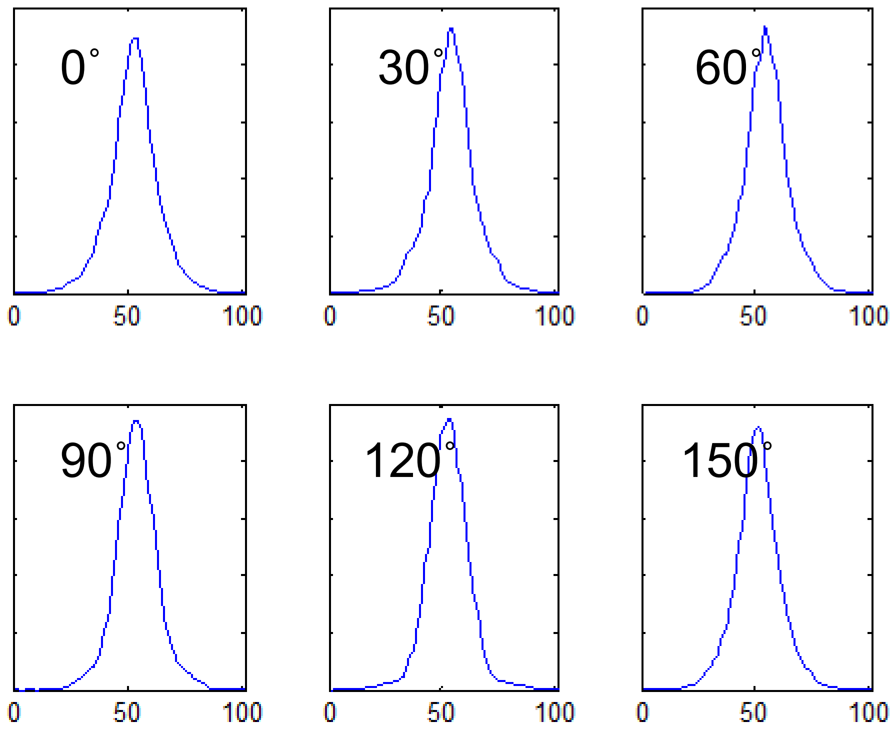

TEST IMAGE

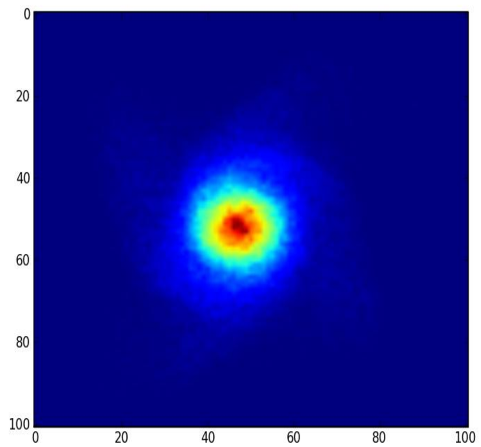

I HAVE

Step 2

Construction of the Projection vector " g "

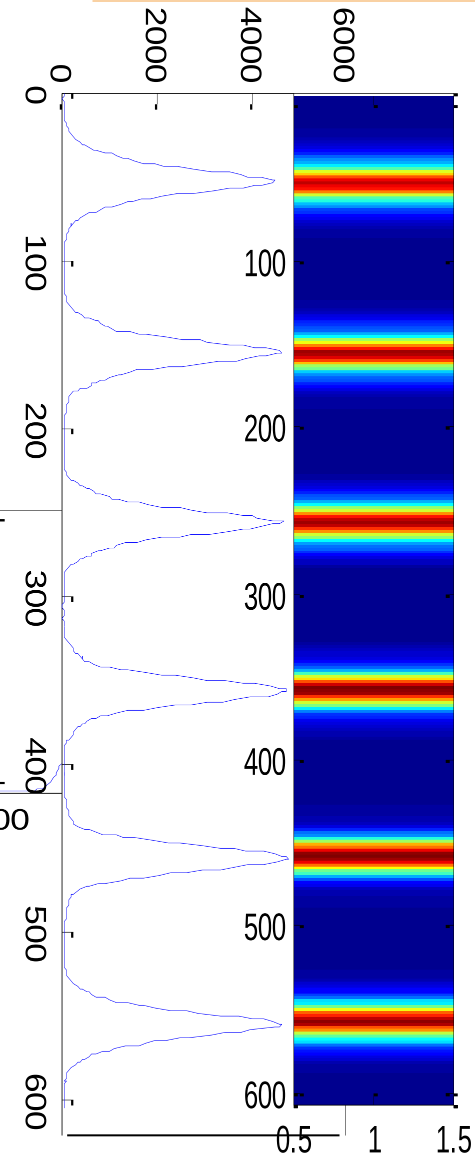

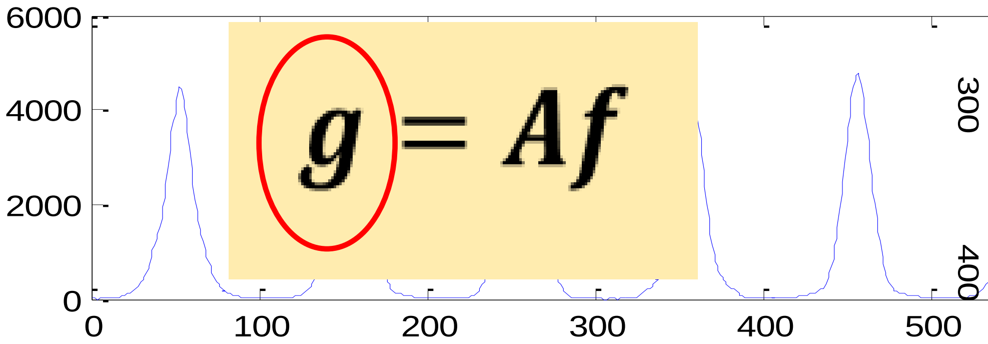

$$g = Af$$

Step 3

Sparse matrix is constructed

$$g = Af$$

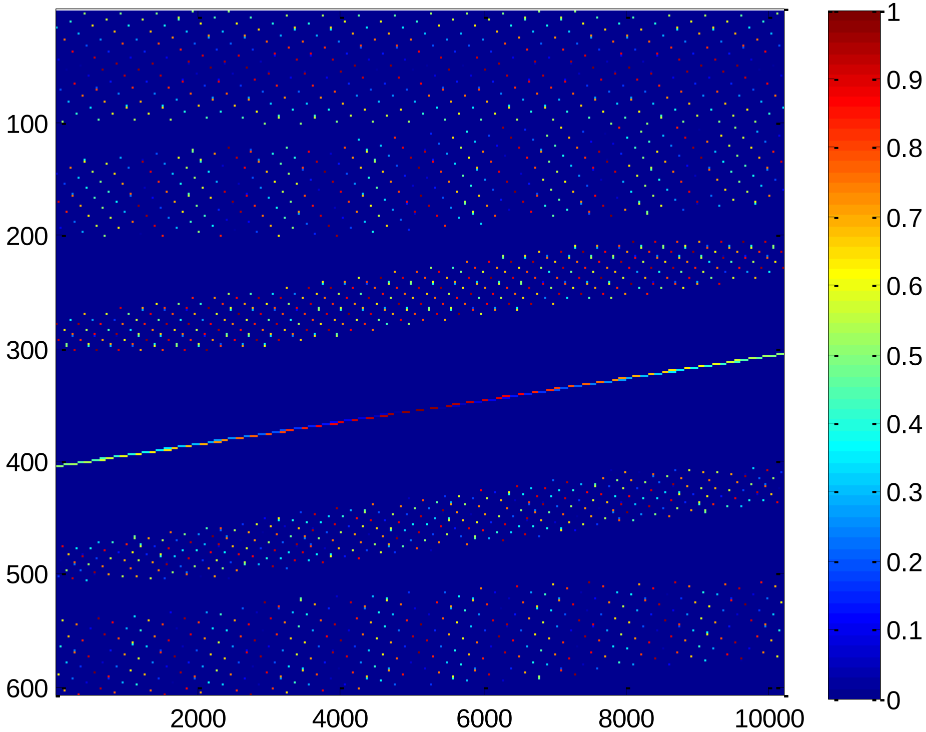

6 projections
101 x 101 image
➔ 606 x 10201 sparse matrix size

Step 4

Must solve for f

$$g = Af$$

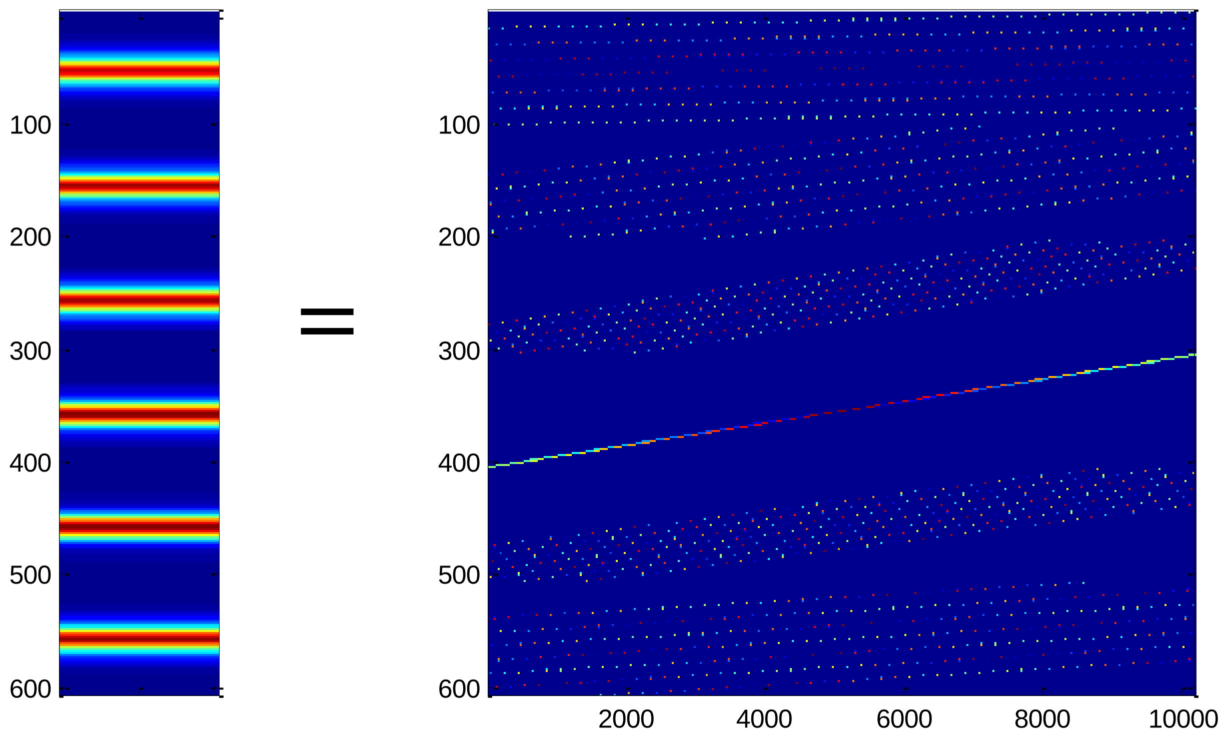

$$\begin{bmatrix} f_1 \\ \vdots \\ \vdots \\ \vdots \\ f_{(101)^2} \end{bmatrix}$$

Step 5, iteration 2

f is reshaped to *101*× *101* image matrix

$$g = Af$$

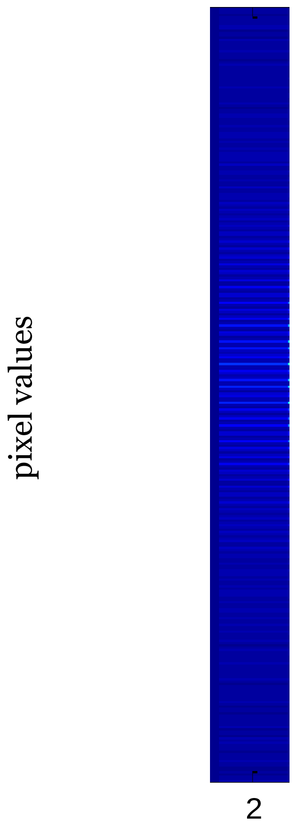

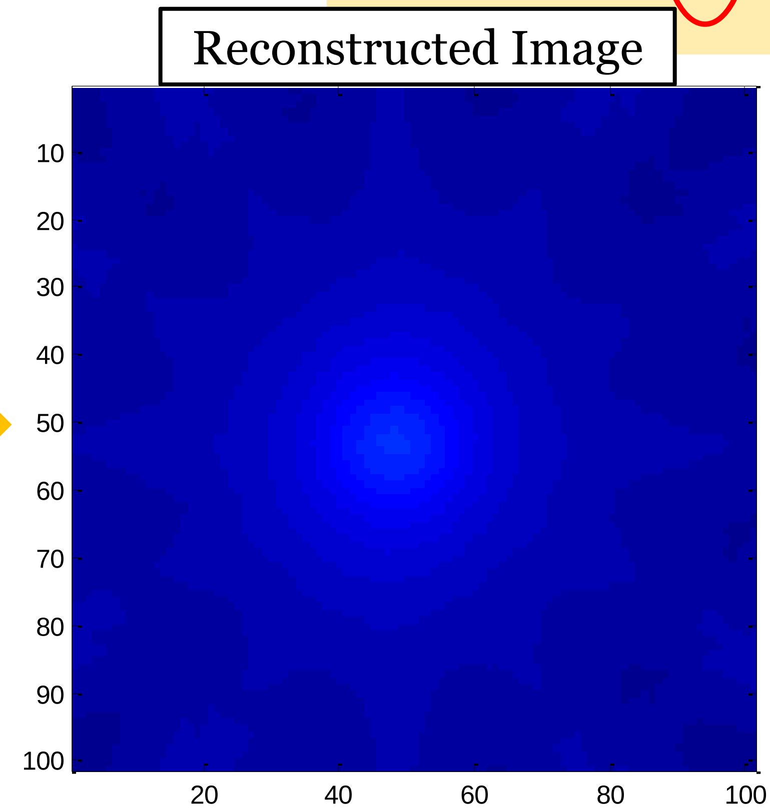

An Illustration

f is solved iteratively

$$g = Af$$

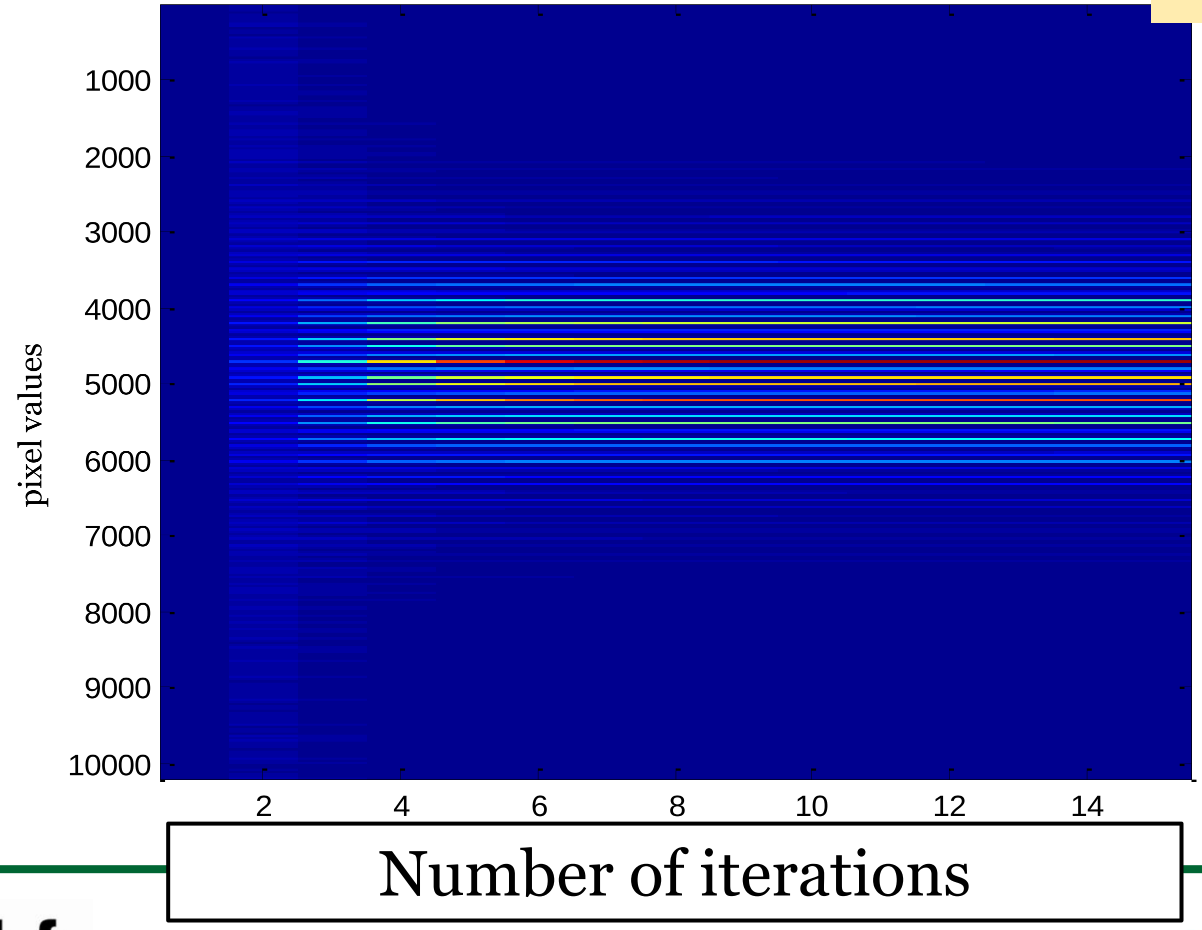

An Illustration

Reconstructed images with respect number of iterations

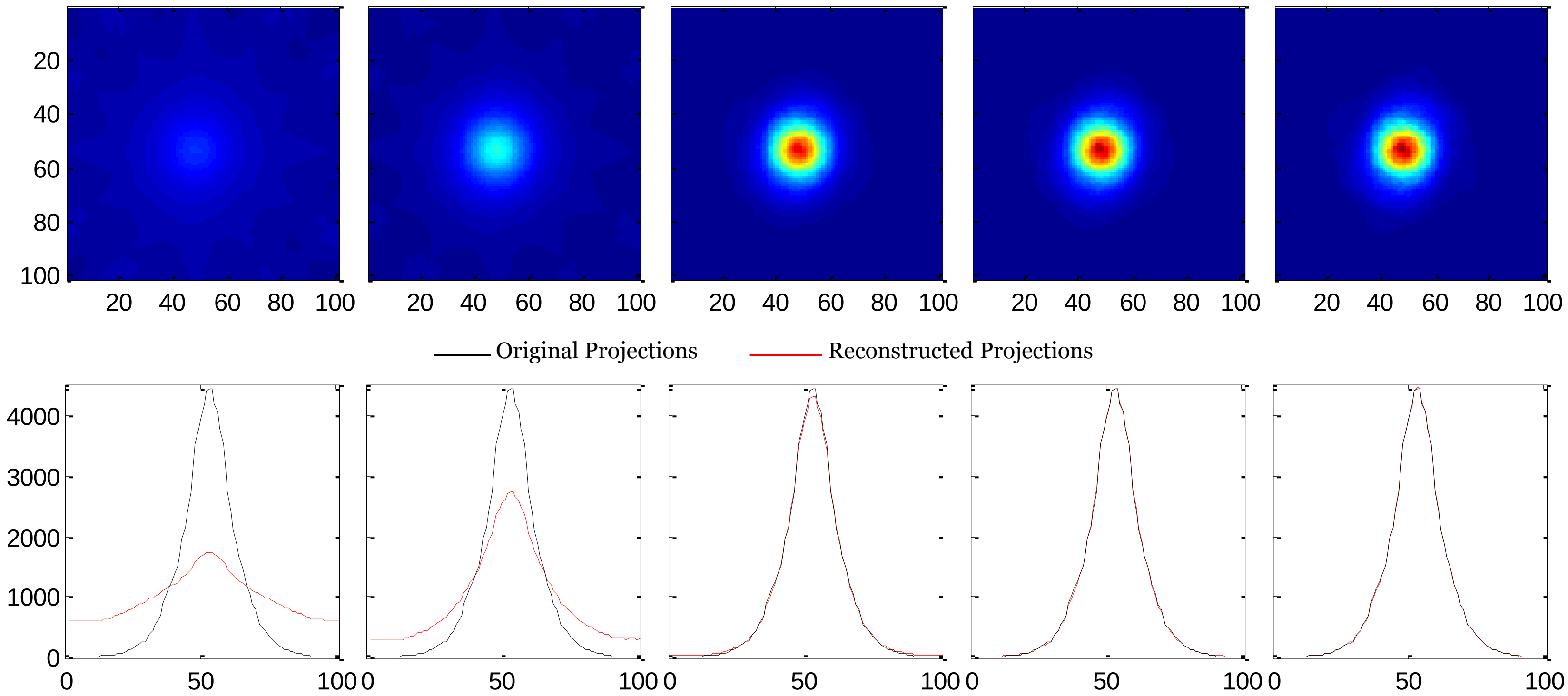

It .2 It.3 It.6 It.8 It.15

Projections measured at 90°

An Illustration

The reconstructed image after 15 iterations

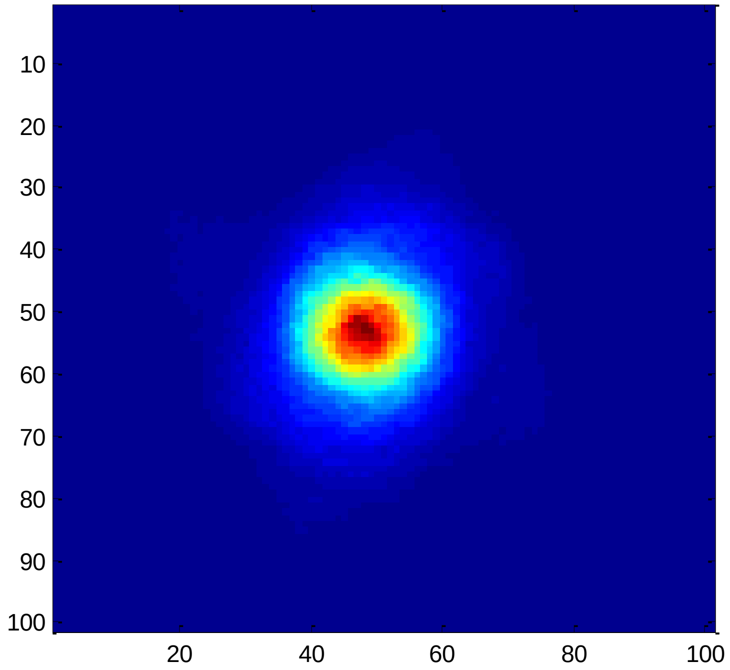

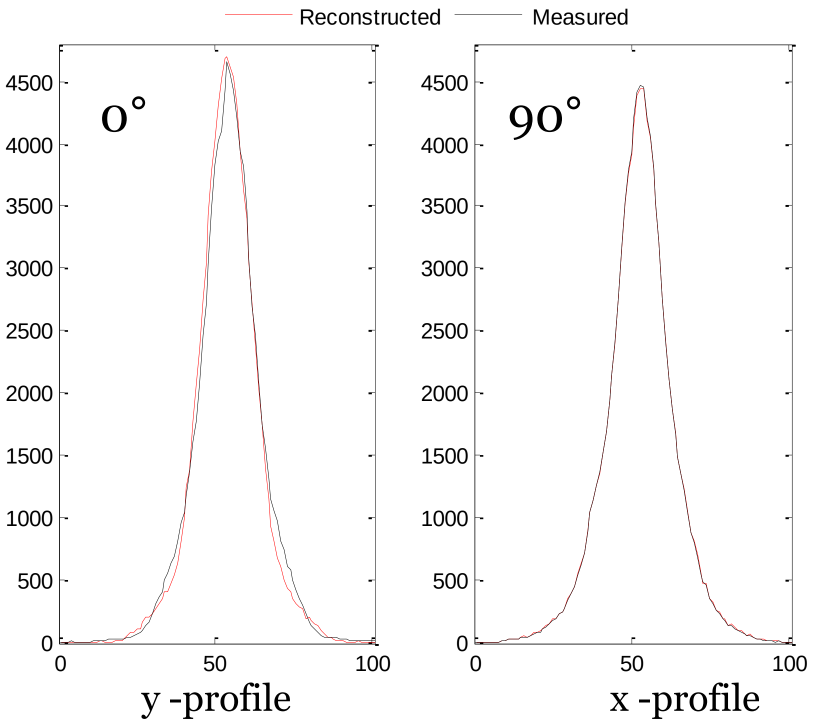

An Illustration

Original image

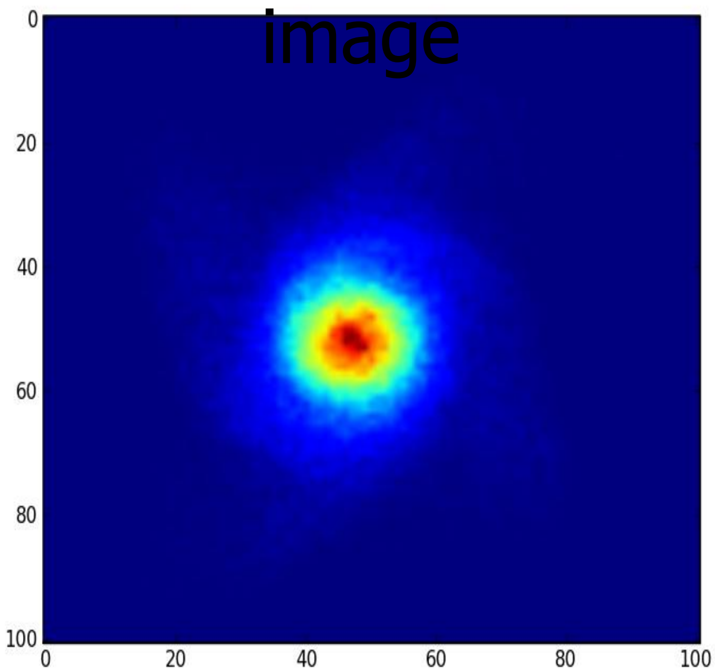

Reconstructed image

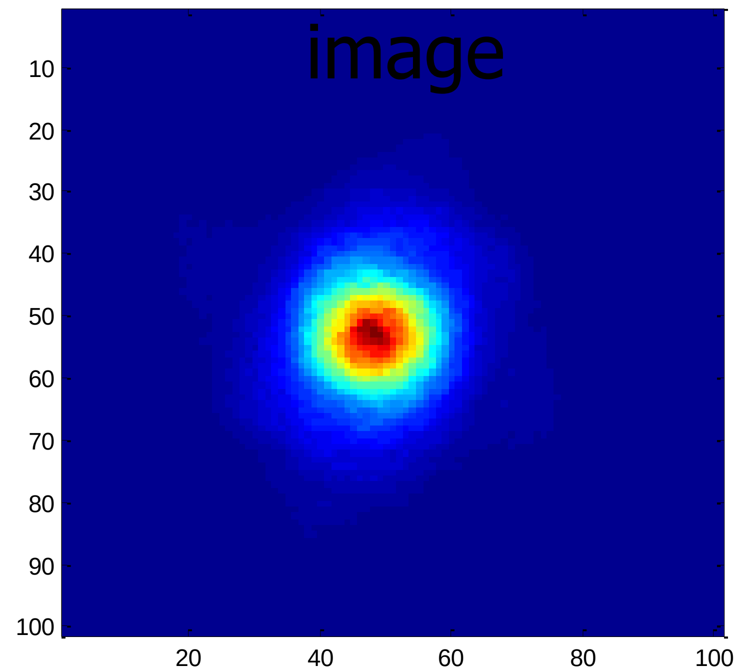

Experimental Measurements With Ion Beams

?

Vacuum Chamber specially designed for Measurements

Spatial density reconstruction

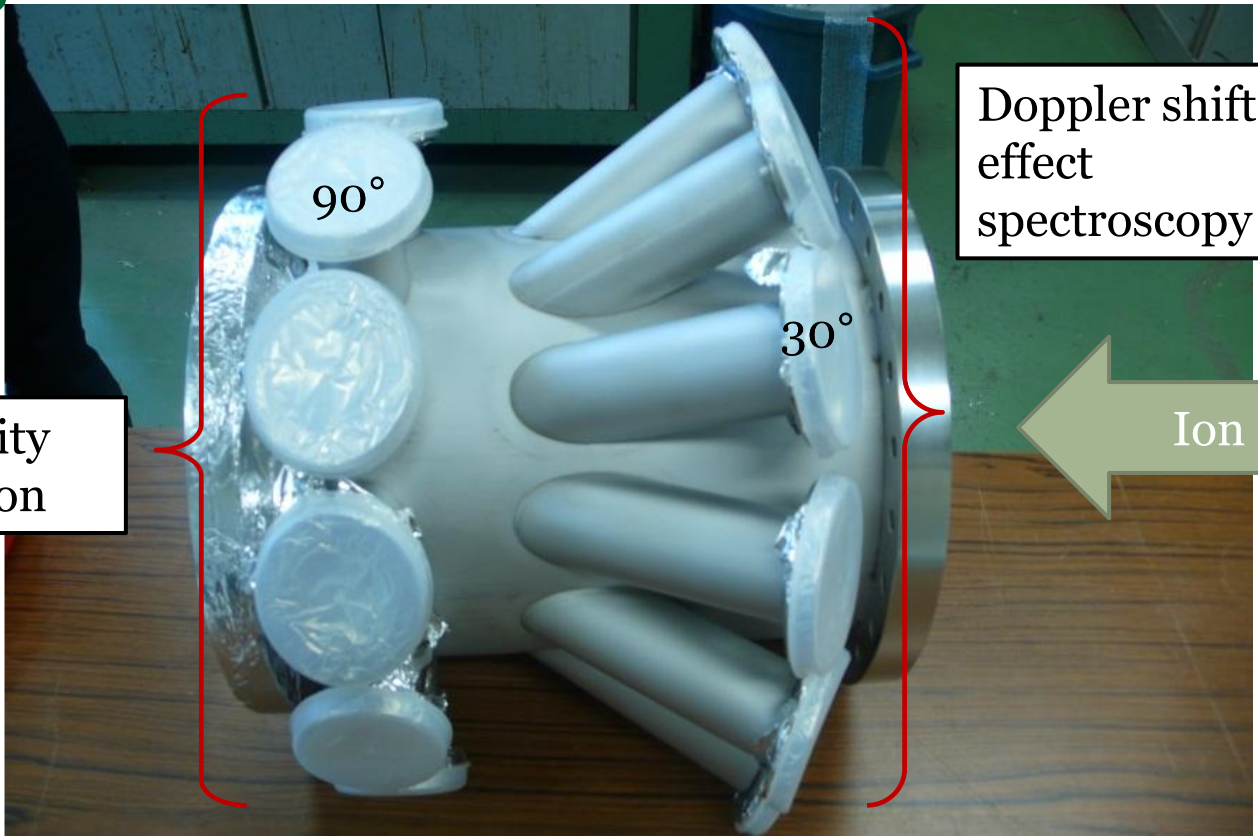

Doppler shift effect spectroscopy

Ion Beam

Imaging and Detection

Focal Length (mm)		25
Iris Range		F1.4 ~ F16
Operation	Focus	Manual
	Iris	Manual
Angle Of View (H×V)	2/3"	19°58′ × 15°02′
	1/2"	14°35′ × 10°58′
	1/3"	10°58′ × 8°14′
Focusing Range (From Front Of The Lens) (m)		∞ ~ 0.15
Object Dimensions at M.O.D. (H×V) (mm)	2/3"	53 × 40
	1/2"	38 × 29
	1/3"	29 × 22
Back Focal Distance (in air) (mm)		14.58
Exit Pupil Position (From Image Plane) (mm)		−32
Filter Thread (mm)		M25.5 × 0.5
Mount		C
Mass (g)		45

Labview

- Stingray F146B
- Fujinon HF25HA-1B objective

Measurements in BETSI test bench

Banc d'Etude et de Tests des Sources d'Ions

ECR SOURCE

Focusing solenoid

Analyzing Magnet

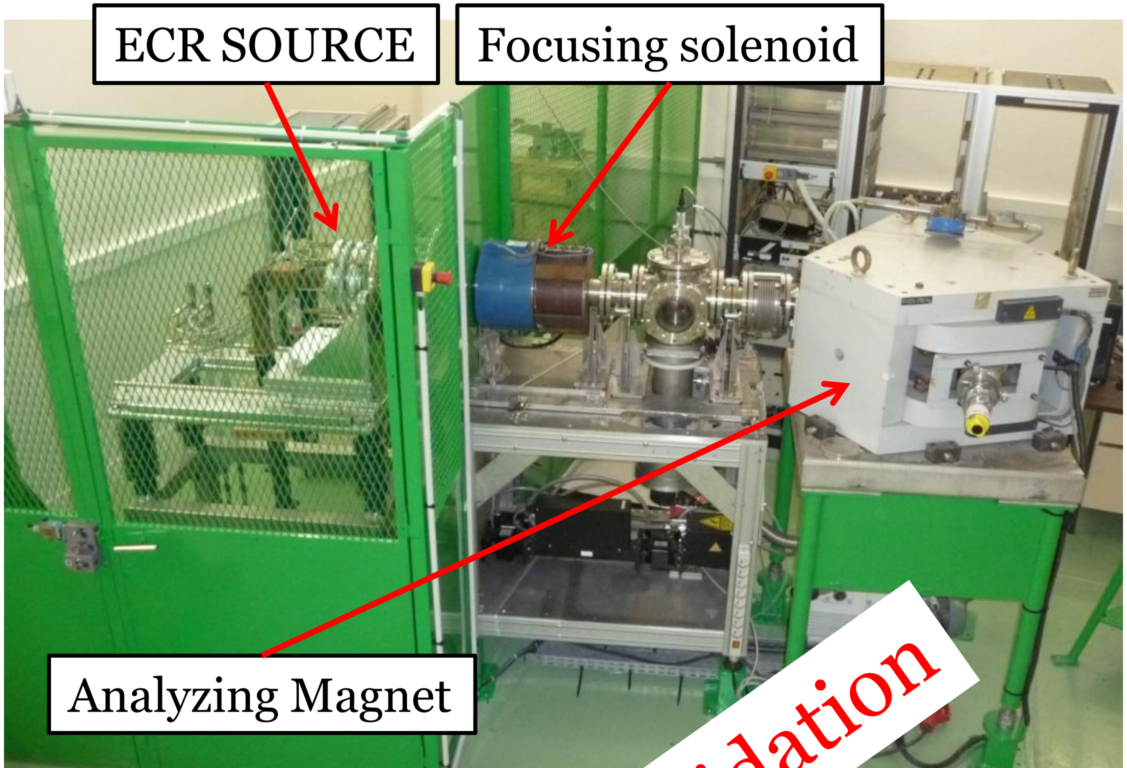

Tomographic chamber after the Magnet

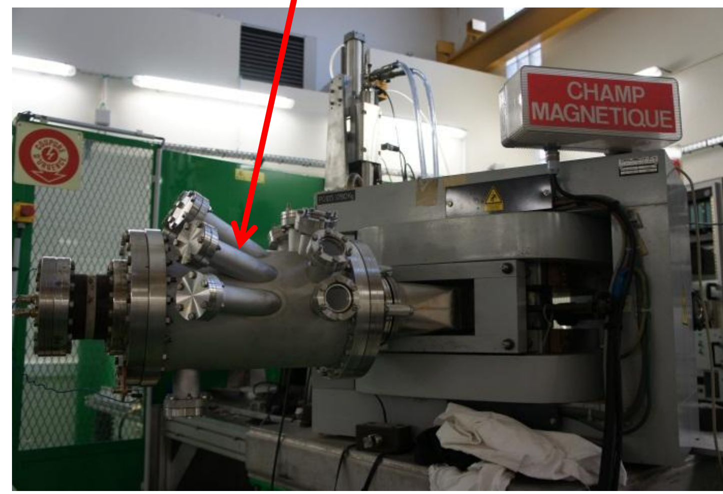

For validation

ECR source
H_2 dominated residual gas
Low Intensity beams : 2mA
H+ current at the beam stop

Measurements in BETSI

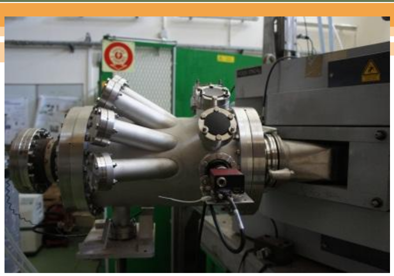

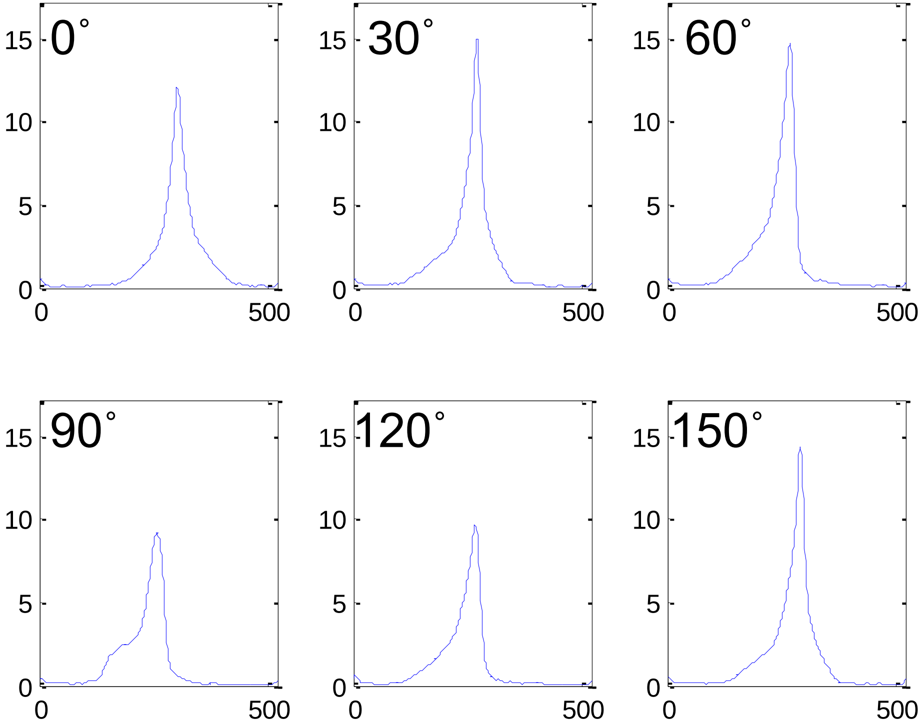

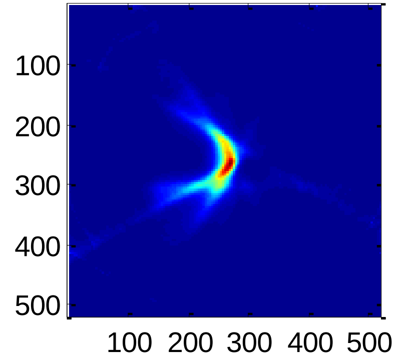

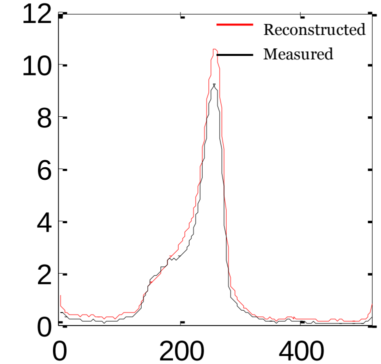

Bizarre"BANANA" shape beam !
NEED MORE VALIDATION

Measurements in SILHI

High Intensity Light Ion Source

- ECRIS: 2.45 GHz - 875 Gauss.
- CW or pulsed mode.
- up to 130 mA at 95 kV ➔ kilowatt of beam power

Measurements in SILHI

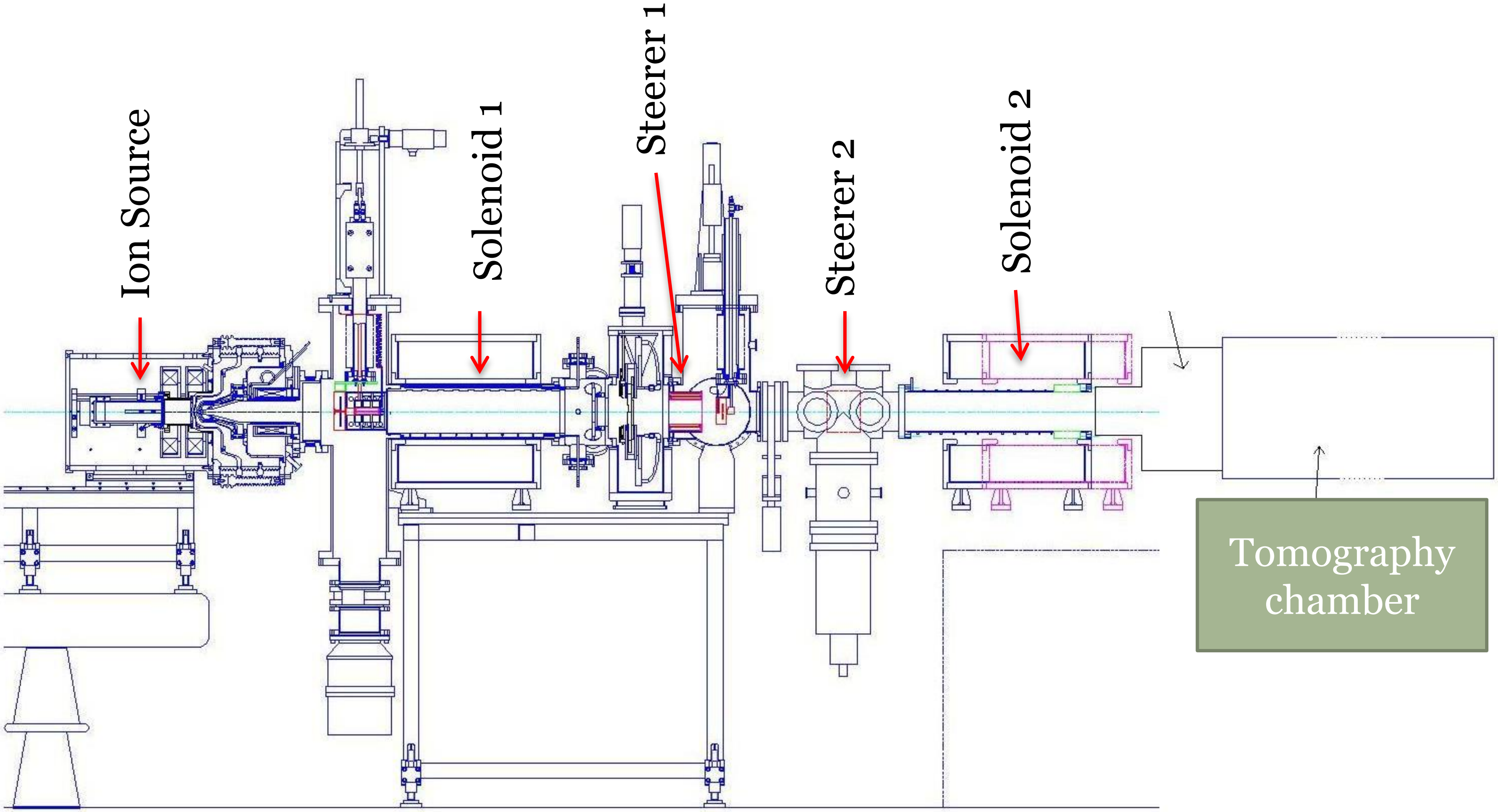

Measurements VS Sol 2 current

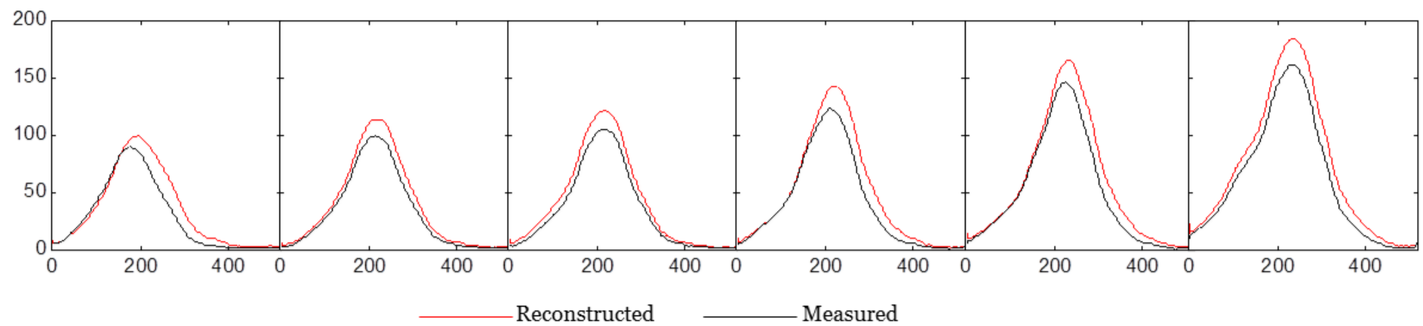

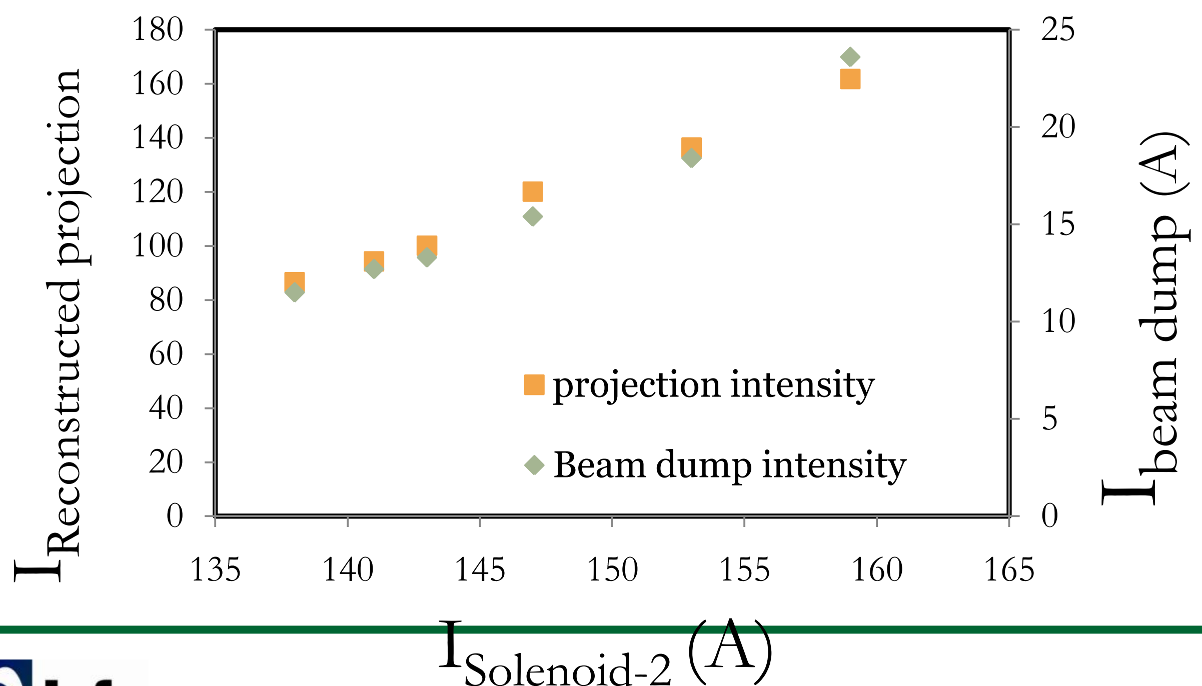

Same Linear dependence of the Intensity of the reconstructed projection at 90° versus the solenoid-2 current as that of the Beam intensity! ✓

Measurements VS Sol 2 current

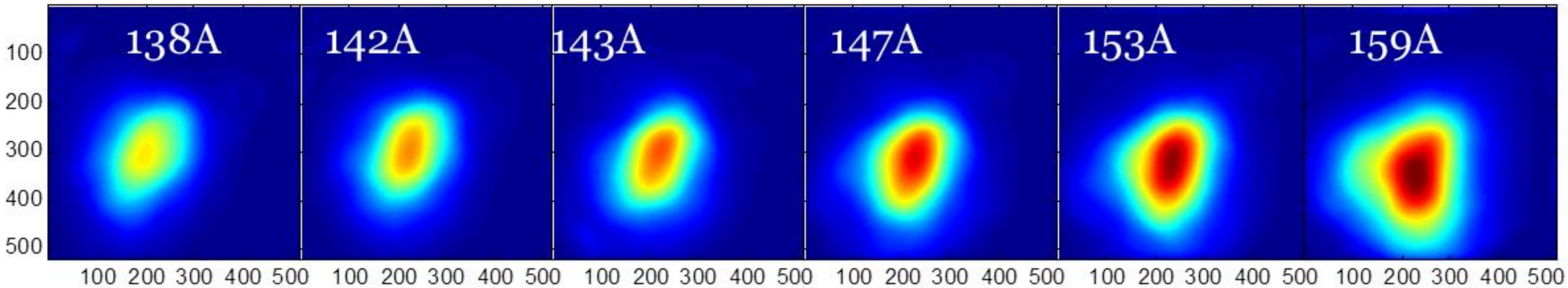

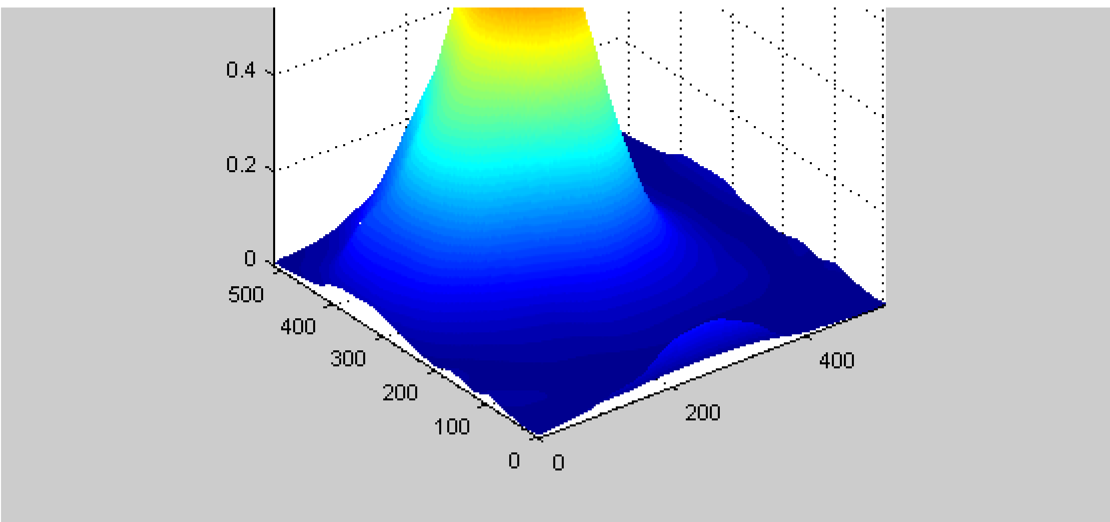

BUT
Beam Shape
Beam position
have changed !

➔ Non linearity of the solenoid for such beam size

Measurements VS Steerer current

Varying the steerer values

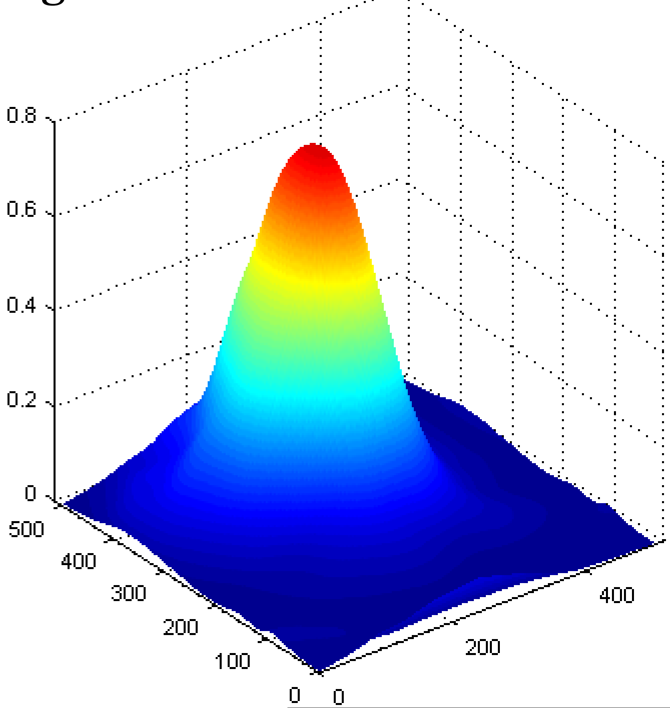

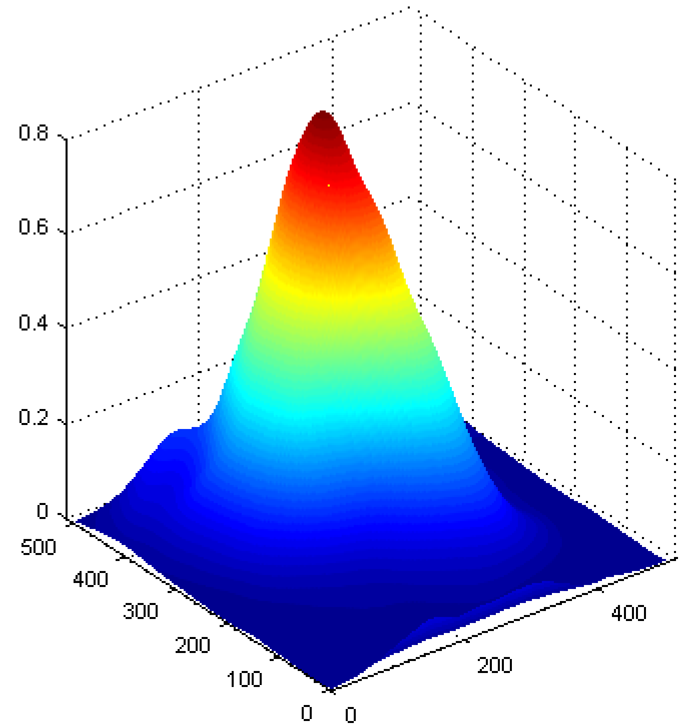

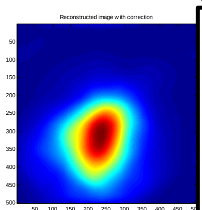

Position has changed ✓
Intensity remains constant ✓
BUT
Beam shape has changed !

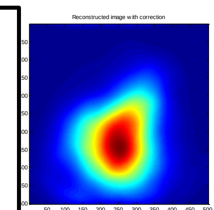

DH1 +0,2
DV1 -0,7
DH2 +0,5
DV2 -0,5

Copper « Profiler »

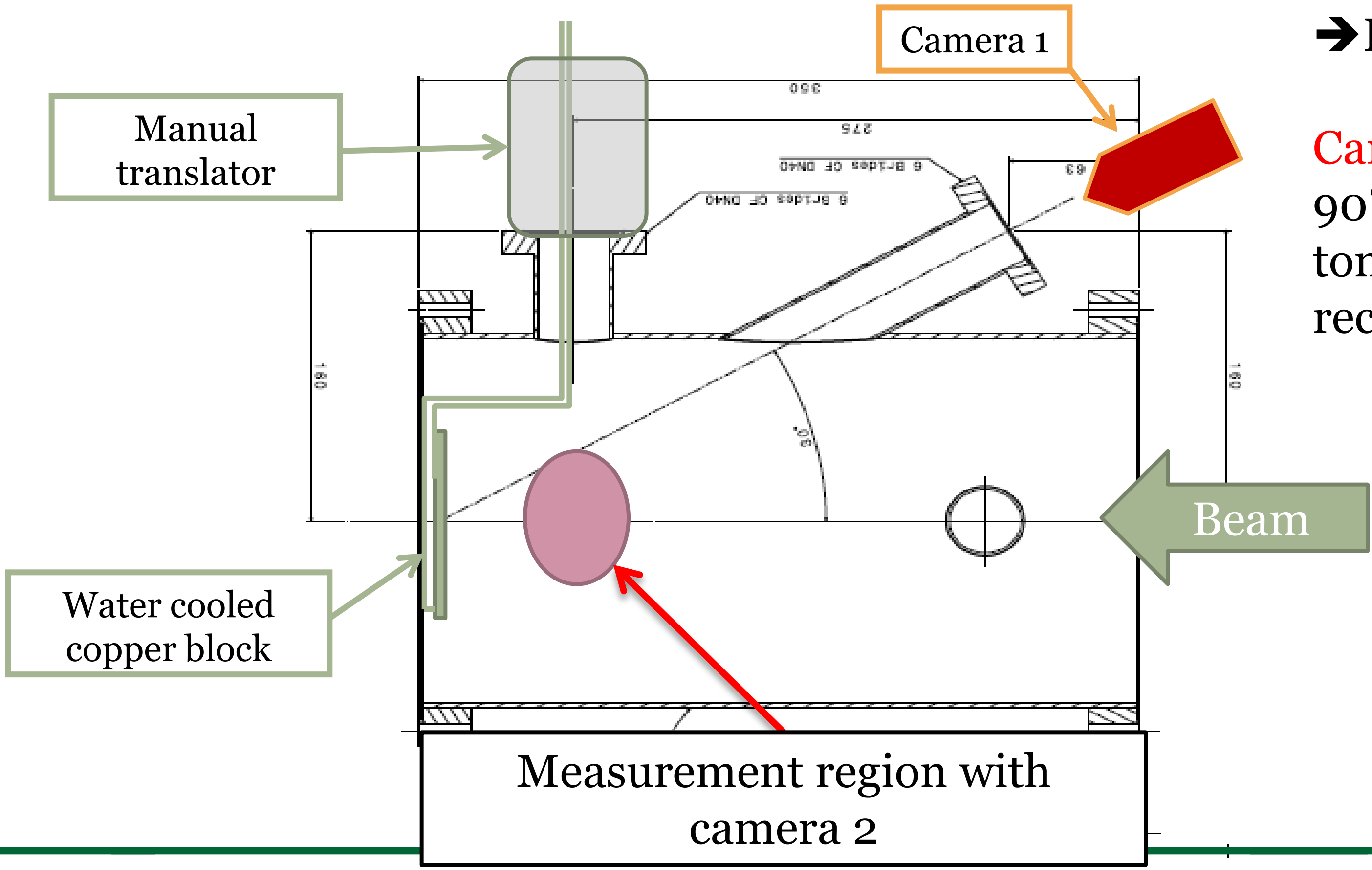

Camera 1 for the copper « profiler » mounted on the 30° viewport
➔BEAM SPOT

Camera 2 on the five 90°-viewport for tomographic reconstruction

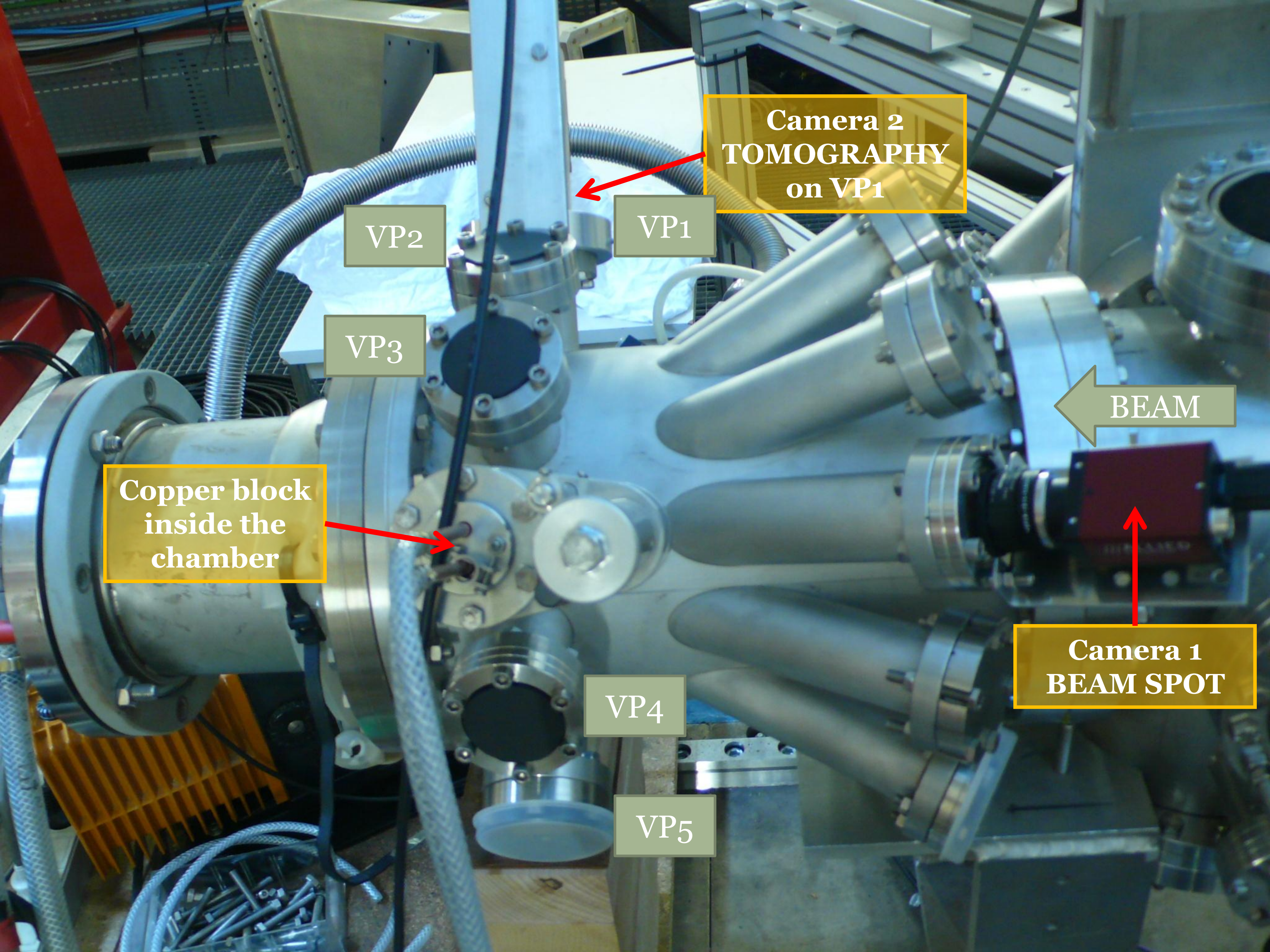
Camera 2
TOMOGRAPHY
on VP1
VP2
VP1
VP3
BEAM
Copper block
inside the
chamber
Camera 1
BEAM SPOT
VP4
VP5

Copper « Profiler »

Comparing the shape of the reconstructed image with 5 viewports with the copper "profiler"

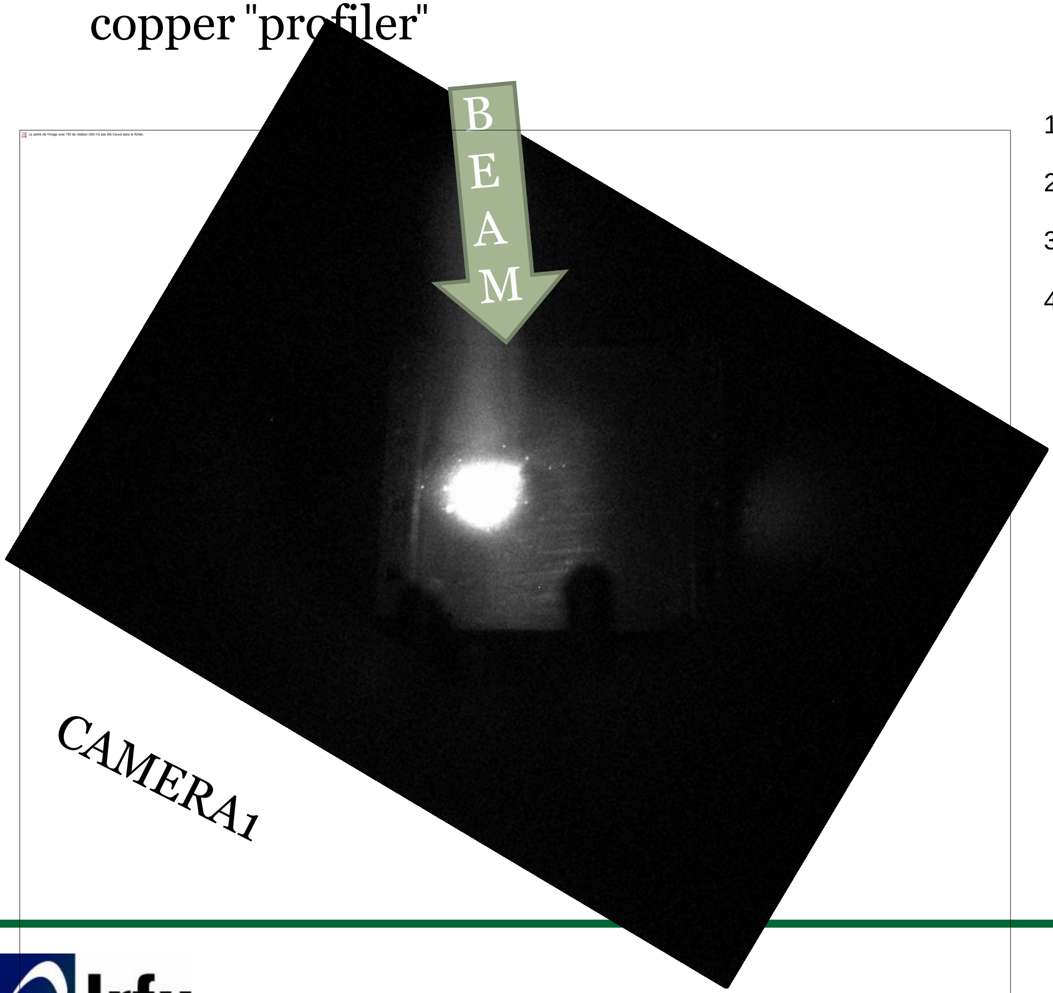

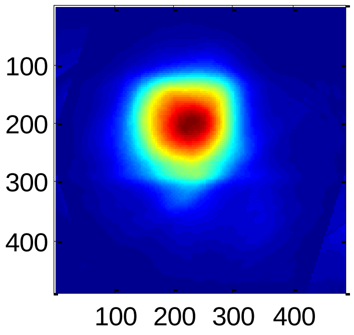

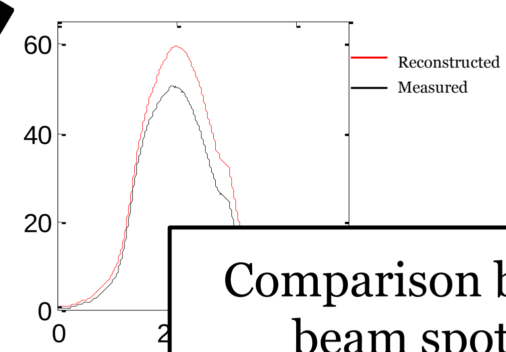

Comparison between the beam spot and the reconstructed image shape is very much comparable even with 5 projections

Conclusion

- It was demonstrated that tomography technique can reconstruct the spatial density of the beam both for low and high intensity beams.
  - 6 viewports seemed to be enough to reconstruct smooth beams.
- The algorithm written in MATLAB is very fast.
  - Future use of 6 simultaneous cameras is foreseen.
- The accuracy of the technique has been verified by comparisons made with copper " profiler" .
  - New comparisons are expected with thermal camera

- Comparison with other algorithm is also expected.
- This algorithm should be VERY useful for the Doppler shift Technique which discriminates different species in the Beam

Acknowledgements

- This work is supported by the DITANET Marie Curie European network.

- Sincere thanks is due to the LEDA group of SACM 🙂

Thank you for your attention